

Development of a deep chlorophyll maximum of *Heterocapsa triquetra* Ehrenb. at the entrance to the Gulf of Finland

Kaisa Kononen,¹ *Maija Huttunen*, and *Seija Hällfors*

Finnish Institute of Marine Research, P.O. Box 33, FIN-00931 Helsinki, Finland

Patrick Gentien

CREMA, BP5, F-17137 L'Hooumeau, France

Michel Lunven

IFREMER, Centre de Brest, BP 70, F-29280 Plouzane, France

Timo Huttula

Pirkanmaa Regional Environmental Centre, PB 297, FIN-33101 Tampere, Finland

Jaan Laanemets, *Madis Lilover*, and *Juss Pavelson*

Estonian Marine Institute, Paldiski Str. 1, 10137 Tallinn, Estonia

Adolf Stips

CEC Joint Research Centre, TP 442 I-20120 Ispra, Italy

Abstract

The development of a deep chlorophyll maximum (DCM) at a depth of 30–35 m was followed during a 15-d case study in July 1998 at the entrance to the Gulf of Finland. The study consisted of three 18–24-h periods of biological (chlorophyll *a*, phytoplankton, primary production), chemical (nitrate, phosphate) and physical (CTD, turbulence, vertical particle size distribution) measurements at an anchor station and six mesoscale towed CTD/fluorometer mappings over the surrounding area. Exceptionally cold and windy weather led to a red tide of the dinoflagellate *Heterocapsa triquetra* instead of the cyanobacterial bloom that frequently occurs in late summer. Comparison of the estimated amount of nitrogen required for an *H. triquetra* bloom biomass with external loading affirmed that the bloom had been formed on the basis of the nitrate pool below the thermocline. The development of the bloom, therefore, led to the extremely deep nitracline. The DCM formed by *H. triquetra* developed at the top of the nitracline at an illumination of <0.1% of the sea surface illumination. A temperature–salinity analysis showed that the DCM was not caused by intrusions from inshore regions. It was concluded that the DCM was formed as a result of changing migratory behavior of *H. triquetra* after an upwelling event that fertilized the upper layer with phosphorus.

One of the keys to understanding population dynamics and species diversity of phytoplankton is resolving hydro-physical and biological mechanisms that allow one species to form a biomass patch in a horizontal or a vertical dimen-

sion. Planktonic organisms live in an environment where light and nutrients, the most important growth-stimulating factors, are vertically separated. Therefore, a species that has the capability to exploit nutrients from depth, but that can simultaneously maintain production, has a competitive advantage over other species that do not have such an ability.

Chlorophyll maximum layers (referred to in the literature as deep chlorophyll maximum [DCM] or subsurface chlorophyll maximum [SCM]) dominated by a single or a few microalgal species have been observed in the oceans, estuaries, and lakes at varying depths, thickness, intensities, and horizontal scales. Important mechanisms of their formation and maintenance include enhanced growth or physiological adaptation in the chlorophyll-rich layer, behavioral aggregation of motile phytoplankton species, sinking and accumulation at pycnoclines, differential grazing, turbulent mixing, internal waves, and horizontal isopycnal intrusions (Cullen 1982 and references therein).

Two different adaptive strategies for producing a DCM

¹ Present address: Academy of Finland, Vilhonvuorenkatu 6, FIN-00500 Helsinki, Finland.

Acknowledgments

We thank the officers and the crew of the RV *Aranda* for their cooperation and flexibility during the cruise. Likewise, our thanks to Susanna Hyvärinen, Pirjo Tikkanen, and Tuovi Vartio for performing nutrient, chlorophyll, and primary production analyses and to Tero Purokoski for operating the CTD. We are grateful to Ants Pastarus and Henry Söderman for the preparation and management of the towed system during the cruise and to Thomas Regelski for improving the language of the manuscript. We also thank John Cullen and an anonymous referee for valuable comments on the manuscript.

The study was funded by the EU MAST3 MITEC, contract MAS3-CT97-0114, and the Maj and Tor Nessling Foundation.

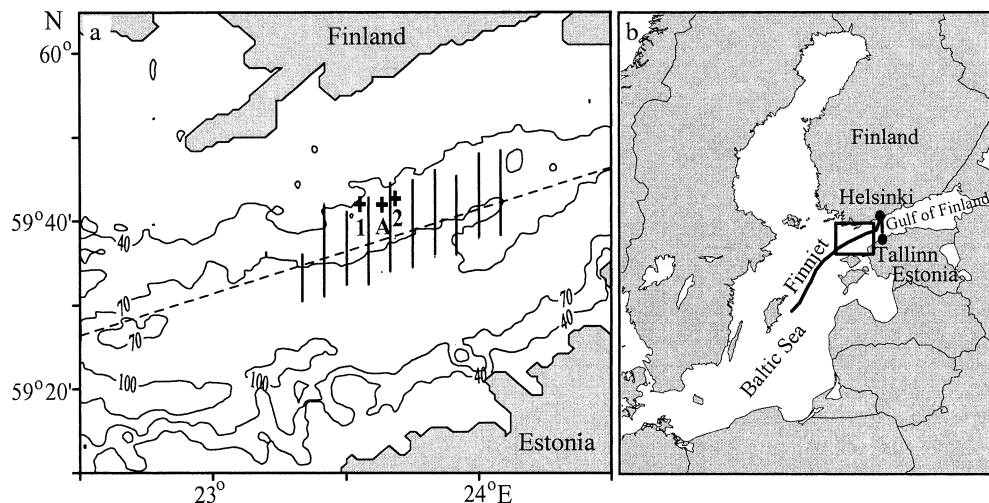


Fig. 1. Map of the study area. (a) The 10 solid lines oriented north–south represent the grid of legs sampled during the towed CTD/fluorometer mappings. The actual mappings consisted of 5–9 successive legs of different lengths. The crosses mark the positions of moorings: 1 and 2, Aanderaa current meters at 8 and 25 m depth; A, the bottom-mounted ADCP. The location of the anchor station coincides nearly with the position of mooring A. The dotted line represents the route of ferry *Finnjet*. Depth contours are given in meters. (b) The bold lines represent the route of ferry *Finnjet* from Helsinki to longitude 20°E and the route of ferry *Wasa Queen* from Helsinki to Tallinn.

have been proposed: layer forming by species that live at low light intensity with high nutrient supply and vertical migration by species that acquire nutrients at depth, where light limits growth rate, then move back to the subsurface layer where nutrients otherwise restrict the accumulation of biomass (Cullen and MacIntyre 1998). In several studies, DCM refers to a chlorophyll maximum located in the thermocline, adjacent to the nutricline, at the bottom of the euphotic layer at the depth where illumination ranges from 0.2–1% (e.g., Venrick et al. 1973; Veldhuis and Kraay 1990; Kononen et al. 1998) to 10% (Mackey et al. 1995) of the surface illumination. Gentien (1998) has also suggested that the DCM of some species results from the optimization of the net growth rate. DCMs formed by the layer-forming strategy typically involve multispecies assemblages, mainly diatoms (e.g., Scharek et al. 1999), picocyanobacteria, and picoeucaryotes (e.g., Agawin and Agustí 1997; Claustre et al. 1999). DCMs formed by the migration strategy, however, are generally composed of single, motile species (mainly dinoflagellates) or of species with buoyancy regulation (cyanobacteria). Also, there are dinoflagellate species that form persistent DCM layers near the nitracline (e.g., Eppley et al. 1984; Cullen and Horrigan 1981).

DCMs have been observed in darkness well below the level of illumination where photosynthesis can occur (i.e., in illumination $<0.1\%$ of the sea surface). For example, Washburn et al. (1991) observed a DCM that was created by purely physical processes through subduction of surface water.

In the Baltic Sea, the term DCM refers to a chlorophyll maximum well below the euphotic layer, as observed by Derenbach et al. (1979) and Pavelson et al. (1999). The term SCM is used for the chlorophyll maximum observed in the lower part of the euphotic layer (e.g., Kononen et al. 1998). Kuosa (1990) and Carpenter et al. (1995) reported on SCMs

formed by dinoflagellates. The mechanism of the formation of these SCMs remained unsolved. In this paper, the formation and maintenance of a DCM at the depth of 30–35 m was studied during a 15-d research cruise at the entrance area to the Gulf of Finland.

Materials and methods

Study site and research strategy—Measurements were made aboard RV *Aranda* (Finnish Institute of Marine Research) from 13 to 27 July 1998 at the entrance to the Gulf of Finland (Fig. 1). The Gulf of Finland is a shallow and elongated basin (the length is ~ 400 km, the width varies from 48 to 135 km). Large river inflow causes surface layer salinity to decrease from 6–7 at the entrance to ~ 1 in the easternmost area (the estuary of the river Neva). Bottom salinity reaches values up to 10 at the entrance to the Gulf. The seasonal thermocline is usually at the depth of 10–20 m and is strongest in July–August when the temperature differences between the layers are 12–18°C. The thermocline effectively restricts the diapycnal mixing of nutrients from nutrient-rich deeper water into the near-surface layer. The long-term circulation in the western Gulf is cyclonic; consequently, the saltier water of the northern Baltic proper intrudes along the Estonian coast, and seaward flow of fresher gulf water occurs at the opposite coast. The entrance area is characterized by high spatiotemporal variability of hydrographic parameters, plankton, and nutrients that is caused by the water exchange between the inner Gulf and the northern Baltic proper, as well as by the local effect of mesoscale phenomena (e.g., eddies, coastal jets, and upwelling/downwelling events). Westerly wind events nearly parallel to the Finnish coast favor upwelling, which brings nutrients (mainly phosphate) into the upper layer.

Table 1. Date and duration of the mesoscale surveys and anchor station studies, the number of CTD profiles measured, sampled profiles taken for nutrient analyses and biological investigations, and turbulence profiles and duration of the series.

	Date (July)	Duration (h)	CTDF (casts)	Nutrients (profiles)	Biology (profiles)	MSS (profiles/ hours)
Survey 1	13–14	18	421	—	—	—
Anchor 1	14–15	21	7	5	3	80/13
FT*	15–16	23	—	35	—	—
Anchor 2	17	24	19	12	6	102/16
Survey 2	17–18	10	224	—	—	—
Survey 3	19–20	17	379	—	—	—
Anchor 3	21	24	20	14	5	96/14
Survey 4**	22–23	11	247	—	23	—
Survey 5	23–24	11	241	—	—	—
Survey 6	26–27	16	339	—	—	—

* Because of heavy weather conditions, only nutrient samples were collected with the FT system at 5 m depth.

** Samples for *H. triquetra* counting were collected with the FT system at 5 m depth.

The study consisted of samplings at the anchor station and mesoscale mappings using a towed undulating system that resolves background hydrographic and chlorophyll *a* (Chl *a*) fields (Table 1). At the anchor station (59°42.5'N, 23°38.0'E), three measurement periods of 21–24 h were carried out involving CTD, water sampling, in situ video recording and particle counting, and microstructure/turbulence profiling. In addition, a cross-shore section with five sampling stations along 23°38.0'E was performed on 16 July. Six CTD/Chl *a* fluorescence mappings were also carried out. During surveys on 15–16 and 22–23 July, water samples were taken from the ship's flow-through (FT) system from the depth of 5 m. Two moorings with Aanderaa RCM7 current meters at 8 and 25 m depth (1: 59°42.3'N, 23°33.6'E; 2: 59°44.1'N, 23°41.4'E) and a bottom-mounted ADCP (RDI Narrow Band 600 kHz) at position A (59°42.1'N, 23°38.1'E) were deployed for the study period (Fig. 1). A bin size of 1 m was used with an integration period of 30 min to obtain better than 1 cm s⁻¹ accuracy for the velocity data. Position A was chosen to be as close as possible to the anchor station.

Background information of the larger scale development of Chl *a* and abundance of *Heterocapsa triquetra* was obtained from the Finnish Algaline (Leppänen and Rantajärvi 1995) along a transect between longitudes 20 and 25°E at the depth of ~5 m (Fig. 1b). Semiquantitative ranking was used according to an abundance scale, where 5 is very abundant, dominant; 4 is abundant; 3 is scattered; 2 is sparse; 1 is very sparse; and 0 is not detected.

Towed CTD/Chl a measurements—The cruise tracks of towed undulating CTD/fluorometer mappings followed 5–9 out of 10 north–south-oriented legs 10–20 km long and 4.6 km apart (Fig. 1). The towed system carried a NBIS Mark III CTD profiler and an Elektro-Optick Suarez fluorometer. Towing speed and mean undulation speed were ~3.5 m s⁻¹ (7 knots) and 0.4 m s⁻¹, respectively. The depth interval ranged from the sea surface down to ~50 m, whereas the longitudinal spacing between successive profiles was ~600 m. Samples for the calibration of the Elektro-Optick Suarez fluorometer were taken at four or five depths between 0 and 30 m before each mapping (except for one mapping because

of stormy weather). The calibration line generated from all data by linear regression ($r^2 = 0.91$, $n = 23$) was Chl *a* (mg Chl *a* m⁻³) = $-0.596 + 0.0674 \times F$, where F is output of the fluorometer in relative units (0–255). The standard deviation of Chl *a* samples about this regression was ± 0.39 mg Chl *a* m⁻³. The large scatter in fluorometer calibration was partly caused by diel variation in the in situ fluorescence yield in the near-surface layer and dark fluorescence of *H. triquetra* (see Fig. 11). In addition, the spatial distribution of species and chlorophyll were very patchy, and because mappings covered a large area (30 × 20 km), we used the single calibration line for towed fluorometer data. All chlorophyll profiles were examined, and obvious spikes were removed by applying a five-point median filter in combination with fixed criteria for spike amplitude. For the drawing of sections and maps, chlorophyll concentration values and CTD data were linearly interpolated at 0.5-m intervals. The raw fluorometer output data, having an average vertical resolution of about 30 cm, were used when resolving the DCM.

Sampling and measurements at the anchor station—During the studies at the anchor station, CTD and fluorescence were measured every hour or second hour. Chl *a* concentration was measured as fluorescence with a fluorometer (Sea Tech) mounted on a SeaBird 911Plus CTD profiler. The Sea Tech fluorometer was calibrated for each measurement series at the anchor station. At the same time, a specific profiler was used to measure vertical particle size distribution. This profiler was composed of a SeaBird 911Plus CTD probe with Seatech fluorometer associated with a particle size analyzer (PSA) as described in Gentien et al. (1995). This system measures the vertical profile of temperature, salinity, photosynthetically available radiation (PAR), in vivo fluorescence, and quantity of particles in the range 0.7–400 μm, as well as their contribution in volume to 30 classes (upper diameter limit: 0.7, 0.9, 1, 0.1, 1.7, 2, 2.6, 3.2, 4, 5, 6, 8, 10, 12, 15, 18, 23, 30, 36, 45, 56, 70, 90, 110, 135, 165, 210, 260, 320 and 400 μm). All data, together with the tape recorder time code, were synchronized and visualized on deck in real time every 2 s.

Because particles are not homogeneously distributed in

seawater and because the volume of measuring cells do not allow robust estimations of particles (fluorescing or not), the profiler was lowered in intervals of at least 1 min; that is, 30 samples were taken in the 8.5-ml measuring cell of the PSA and in the small (<1 ml) measurement volume of the fluorometer.

Measurements of turbulence were carried out with the microstructure measuring system (MSS) (Prandke and Stips 1998) in hourly series of five to seven casts in series. The MSS profiler was equipped with shear probe and CTD sensors to obtain a high-resolution hydrographic background. From shear data, the viscous dissipation rate of turbulent kinetic energy, ε , was calculated as described in Prandke and Stips (1998). Considering the errors in the estimation of ε (Moum and Lueck 1985), the accuracy of ε at the levels above $10^{-9} \text{ W kg}^{-1}$ was within a factor of two. Based on the Osborn (1980) model, the vertical eddy diffusion coefficient K for mass was estimated as $K = 0.2\varepsilon \times N^{-2}$, where N^2 is the buoyancy frequency squared.

The vertical turbulent chlorophyll flux ($\text{Chl } a_{\text{flux}}$) was calculated as $\text{Chl } a_{\text{flux}} = -K \partial(\text{Chl } a)/\partial z$, with the z -axis positive upward. The ε , density, and chlorophyll data were merged on a 1 m/1 h grid. Before finally calculating K and $\text{Chl } a_{\text{flux}}$, the data were filtered with a low-pass Butterworth filter having a 4 m/2 h cutoff. The vertical derivatives of density and $\text{Chl } a$ concentration were calculated by their central differences. To avoid the disturbances caused by the ship that falsify ε , only data below 12 m depth (which is more than twice the ship draught) were used.

Nutrient samples were taken with a Rosette sampler from depths of 5, 10, 15, 20, 22.5, 25, 27.5, 30, 32.5, 35, 37.5, 40, and 50 m. Samples for the high-resolution determination of nutrients, phytoplankton, and $\text{Chl } a$ from the DCM were taken with a 3-m-long decimeter-scale sampler. The sampler is equipped with two parallel arrays of 30 plastic syringes, each with a volume of 100 ml and located at 10-cm intervals in the metal frame. The sampler was operated hydraulically, which ensured smooth and simultaneous sampling by all syringes.

Phosphate and nitrate concentrations were determined according to the guidelines for the second stage of the Baltic Monitoring Programme (BMEPC 1983). Primary production was measured by adding $1.4 \times 10^5 \text{ Bq}$ ($3.7 \mu\text{Ci}$) as $\text{NH}_4^{14}\text{CO}_3$ to 60-ml samples taken from the DCM. Samples were incubated 2 h both in situ and at 3 m depth. After incubation, inorganic ^{14}C was removed by adding HCl, and the radioactivity in the total sample was measured.

Samples for quantifying phytoplankton species (50 ml) were preserved with Lugol's solution and were counted using the Utermöhl (1958) technique.

Laboratory determination of fluorescence of *H. triquetra*—A strain of *H. triquetra* (KAC25) was kindly provided by C. Legrand (University of Kalmar, Sweden) and grown at 26 psu, 16°C , under $60 \mu\text{mol photons m}^{-2} \text{ s}^{-1}$ on $f/2$ medium. Cell size in the culture was measured with the PSA. To determine the ability of the species to sustain itself and to bloom in darkness, the culture was first grown under full light (18°C , $80 \mu\text{mol photons m}^{-2} \text{ s}^{-1}$), then it was transferred into darkness at 7°C . These conditions nearly corre-

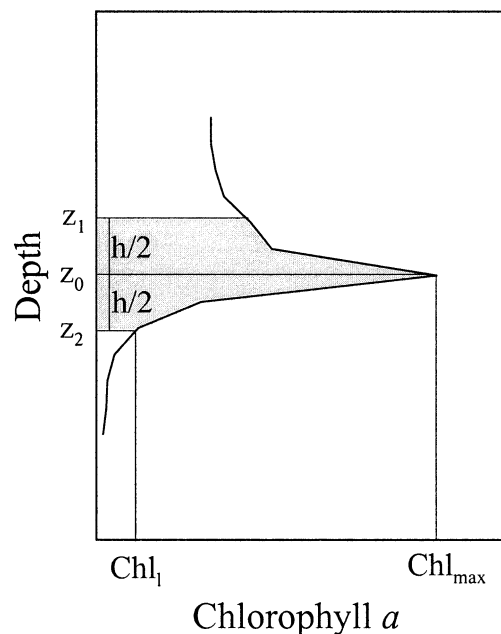


Fig. 2. The schematic diagram of the DCM layer and definitions of the DCM parameters. The depth of the peak value Chl_{max} determines the depth of the DCM (z_0). The DCM temperature and salinity are determined at that depth. The depth of the lower boundary of the DCM layer (z_2) is determined by the depth where the $\text{Chl } a$ concentration value $\text{Chl}_1 = 0.5 \text{ mg Chl } a \text{ m}^{-3}$. The depth of the upper boundary (z_1) and the thickness (h) of the DCM follows from a rough assumption of symmetry of the DCM relative to z_0 . The chlorophyll content (Chl_{con}) of the DCM is the integral over the chlorophyll profile from depth z_1 to z_2 (shaded area).

spond to those observed in the DCM. Cell density, in vivo fluorescence, and chlorophyll concentrations per cell were all followed for a period of 18 d.

Definition of the DCM—The shape of the $\text{Chl } a$ profiles in the layer below the thermocline varied considerably. For statistical analysis, we defined the main DCM parameters (depth of peak value, thickness, chlorophyll content) shown on the sketch in Fig. 2. Chlorophyll concentration of $0.5 \text{ mg Chl } a \text{ m}^{-3}$ was fixed as a lower boundary of the layer, and for the estimation of the upper boundary, the symmetry of the chlorophyll distribution in the DCM relative to the depth of peak chlorophyll concentration was assumed.

Results

Meteorological and hydrophysical conditions during the measurements—Because of cloudy and cold weather in June and the first 10 d of July, the surface temperature remained $\sim 15^\circ\text{C}$. Three atmospheric cyclones passing through the area caused strong wind events from the southwest (14–16 July) and south–southwest (19–21 and 25–27 July) at speeds of $10\text{--}15 \text{ m s}^{-1}$. Despite the strong wind forcing, only a relatively weak upwelling signature was detected in the sea surface temperature after the first wind event. The second and third wind events strengthened the upwelling. On satellite images, the signature of upwelled water was observed along

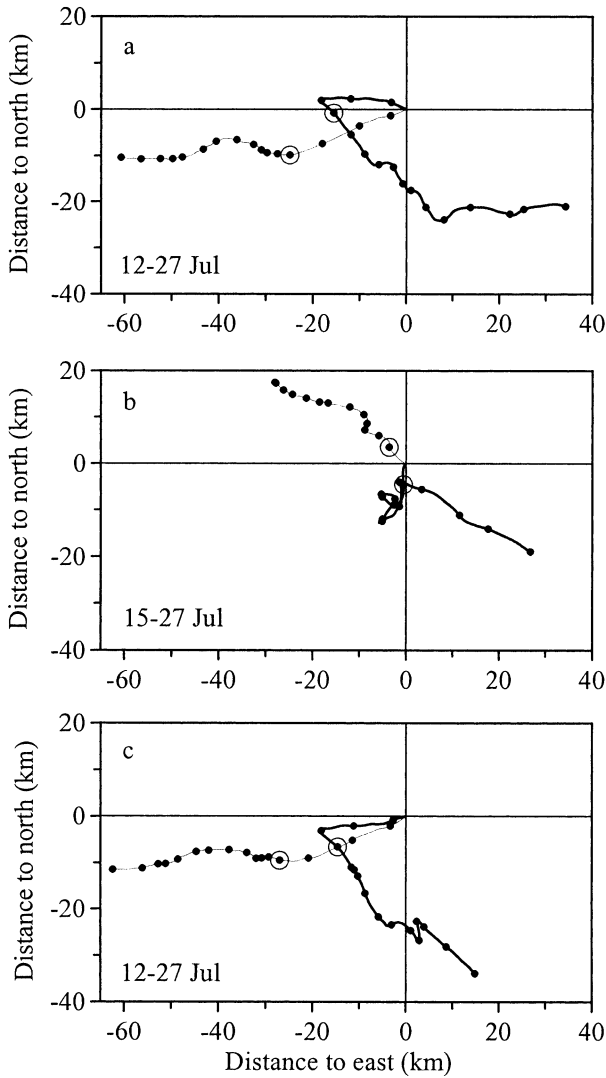


Fig. 3. Progressive current vector diagrams at the moorings (a) 1, (b) A, and (c) 2. The bold lines represent current at 8 m depth. The thin lines represent current at 25 m depth (moorings 1 and 2) and at 30 m depth (mooring A), which correspond nearly to the DCM depth. Dots indicate the beginning of day and circled dots mark 16 July. The inertial oscillations were removed by the use of a 24-h running mean. Note: An east- or westward current speed of about 5 cm s^{-1} is needed to transport water parcels from one leg to the neighboring leg (distance between legs was 4.6 km).

the whole Finnish coast (H. Siegel pers. comm.). As the Baltic Sea is relatively turbid, the mean depths corresponding to 1 and 0.1% surface light intensity (determined from profiles of PAR) were 9 and 16 m, respectively.

A mainly two-layer flow system was observed at all moored current meter locations (Fig. 3). At the start of our measurements, the boundary that separated layers was at the upper part of the seasonal thermocline/pycnocline at a depth of $\sim 10 \text{ m}$ (Fig. 4a). Because of the strong winds, this depth gradually descended, and it was about 10 m deeper by the end of the observation period (Fig. 4b–d). During 14–15 July at the first anchor station, the moderate WSW along-shore current of $8\text{--}12 \text{ cm s}^{-1}$ was observed in the lower layer

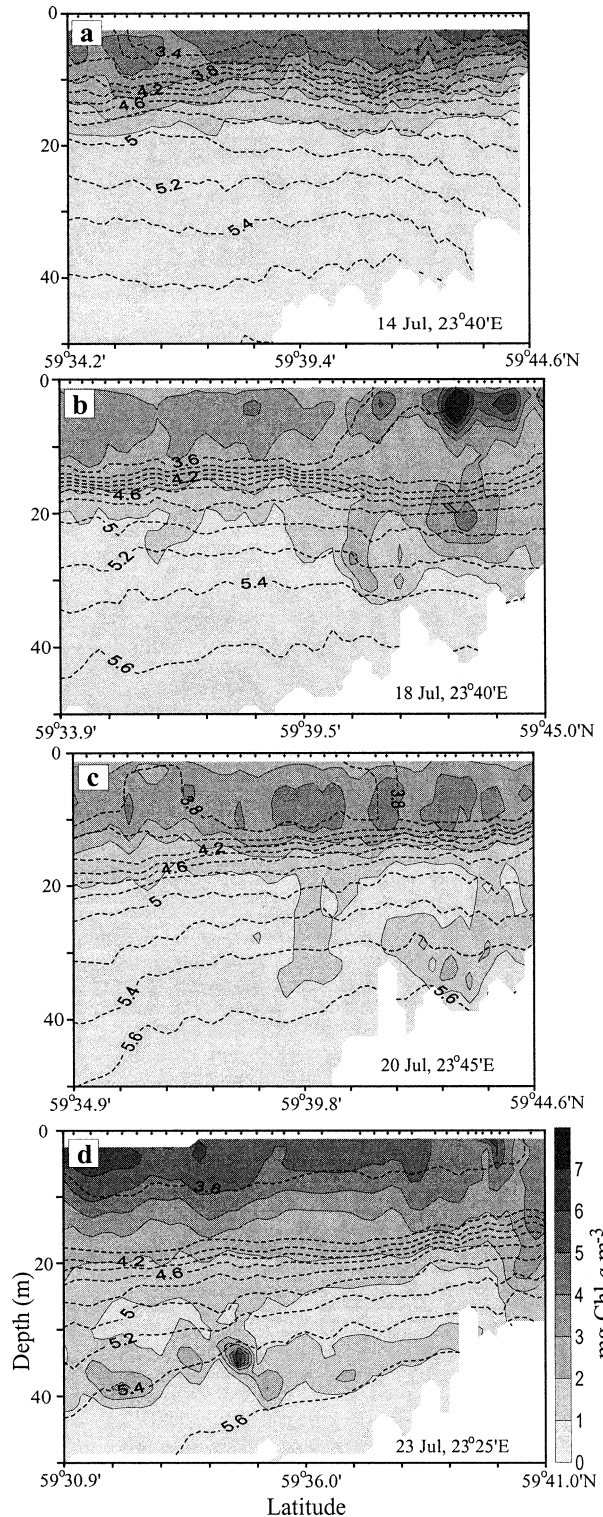


Fig. 4. Meridian vertical distributions of Chl *a* measured during surveys on (a) 14 July, (b) 18 July, (c) 20 July, and (d) 23 July in gray scale at $1\text{-mg Chl } a \text{ m}^{-3}$ intervals overlaid with the isopycnals at 0.2-kg m^{-3} intervals. Vertical ticks in the top of each panel show the location of profiles.

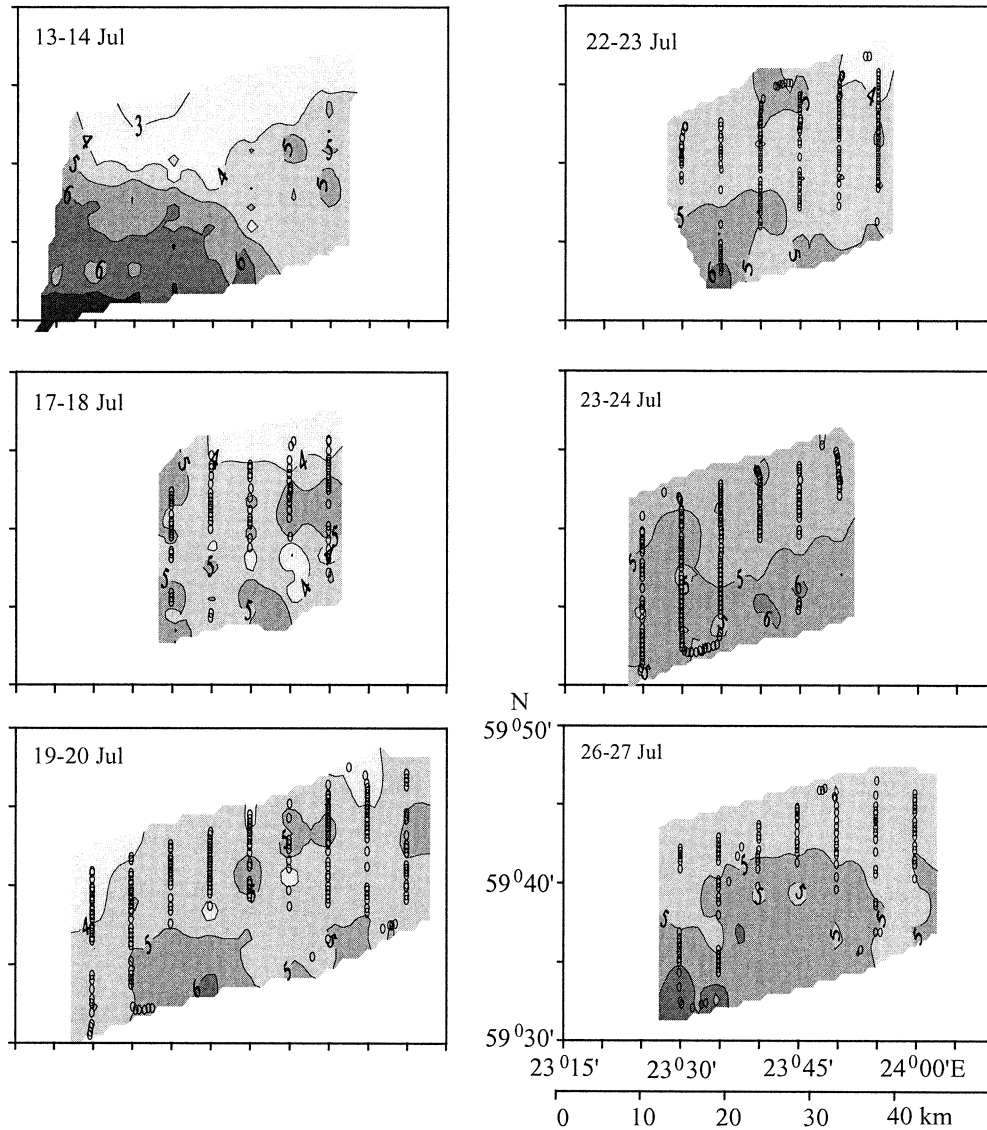


Fig. 5. Maps of the isotherms in gray scale at 1°C intervals on the isopycnal surface of 5.4 kg m⁻³. Circles show the geographic distribution of the DCM layers determined on chlorophyll profiles measured on legs of mapping.

(Fig. 3a,c). On 15 July, the current in the upper layer turned to the SE, while the current in the lower layer weakened (1–5 cm s⁻¹) and continued westward until the end of the observation period. During the second and third anchor station, on 17 and 21 July, respectively, the current speed was very low, ~1–2 cm s⁻¹.

The evolution of water masses is shown on temperature maps on a density surface of 5.4 kg m⁻³ (Fig. 5), which corresponds roughly to the DCM mean density (Fig. 4). On 13–14 July, a strong temperature/salinity front, split into two branches, and a separation of the cold coastal water (<4°C) from the warm water (>6°C) of the northern Baltic proper was observed in the western part of the area. In between these branches, the water temperature was 4.0–5.5°C; this water mass likely originated from the inner Gulf as the westward current dominated. By the time of the survey on 17–18 July, this water had spread over the anchor station to the

western end of the study window. All the following mappings showed the presence of the same water and, in part, the cold water along the coast. In the central area, some cold water patches on a scale of 5–10 km were observed (see 17–18 and 19–20 July) that might be interpreted as intrusions from the coastal zone.

Nutrients—The vertical distributions of phosphate and nitrate concentrations observed at the anchor station were substantially different during the whole sampling period. Nitrate concentration was almost below the detection level from the sea surface down to a depth of ~25 m during the measurements at the anchor station on 14–15 July (Fig. 6a). The top of the nitracline deepened to about 30 m on 17 July and remained close to this depth until the end of the third sampling period at the anchor station on 21 July (Fig. 6b,d).

Phosphate concentration was ~0.03 μmol L⁻¹ in the upper

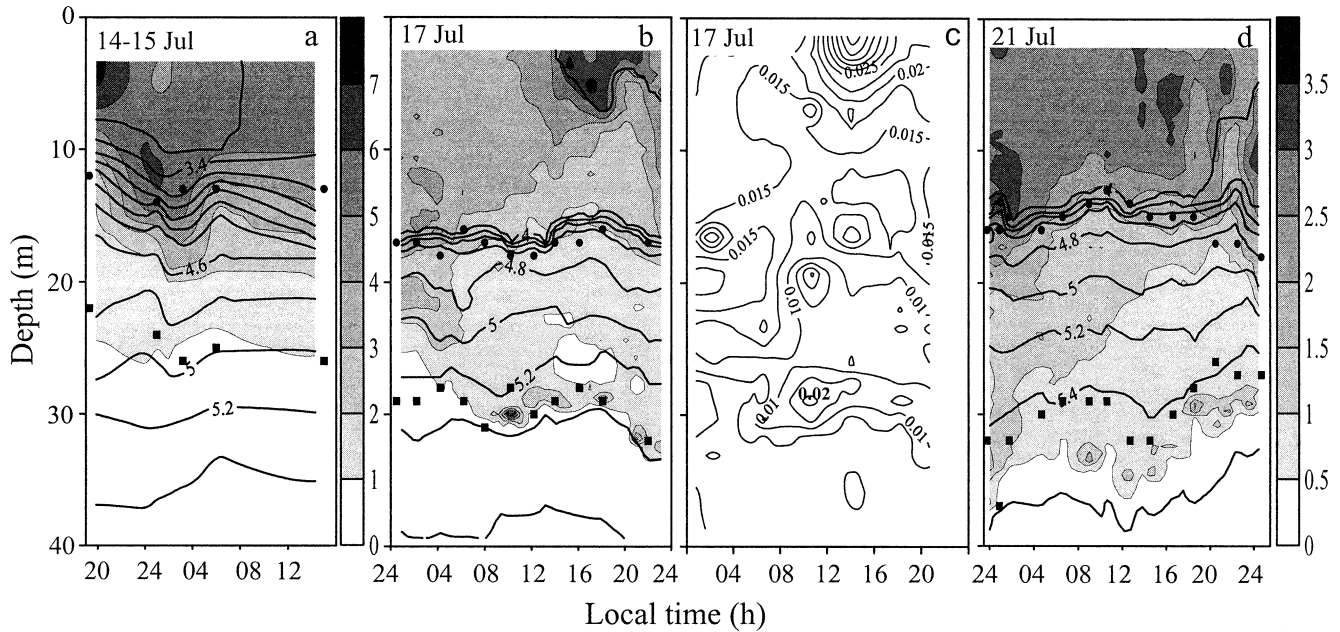


Fig. 6. Vertical distributions of Chl *a* in gray scale at $1 \text{ mg Chl } a \text{ m}^{-3}$ intervals overlaid with isopycnals at 0.2 kg m^{-3} intervals on (a) 14–15 July, (b) 17 July, and (d) 21 July in the anchor station. (c) Vertical distribution of particles in the size range of $18\text{--}30 \mu\text{m}$ at intervals of 0.0025 (in relative units) on 17 July. Filled circles mark the depth of the phosphocline; filled squares mark the depth of the nitracline in panels a, b, and d.

layer, and the top of a smooth phosphocline was located in the thermocline at a depth of $\sim 13 \text{ m}$ on 14–15 July (Fig. 6a). The weak upwelling along the Finnish coast and wind-induced mixing on 15 and 16 July led to an increase in the concentration of phosphate up to $0.1 \mu\text{mol L}^{-1}$ in the upper mixed layer of the northern part of the study area; the concentration remained low in the southern part (Fig. 7). At the

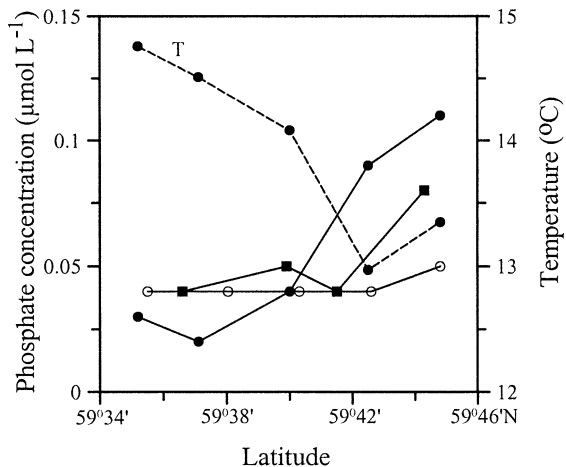


Fig. 7. The distributions of phosphate concentration and temperature along $23^{\circ}38'E$ on 16 July at 5 m depth, demonstrating the wind-forced transport of phosphate inshore into the upper layer. Circles represent the phosphate concentration measured from samples taken during the FT survey between 0300–0500 h local time and filled squares between 0600–0730 h. Filled circles represent phosphate concentration and dashed line with filled circles temperature measured in the sampling stations between 0830–2100 h, after the peak wind speed.

same time that the concentration of phosphate at the surface layer increased, the top of the phosphocline lowered to $\sim 17 \text{ m}$ (Fig. 6b). The phosphate profiles showed frequent maxima at 20–25 m depth (Fig. 8a–c). These phosphate-rich intrusions were above a warmer, saltier, and less phosphate-rich water mass and were likely related to the internal front (see Fig. 5) that separated the inshore, colder, phosphate-rich water from the warmer open Gulf water that contained less phosphate. Similar intrusive layering was not observed in the nitrate and fluorescence profiles (Fig. 8). This means that the intrusions were formed above the nitracline, where the fluorescence levels were almost the same.

Phytoplankton, Chl a, particles, and primary production—The dominant phytoplankton species in the euphotic layer during the observation period were *H. triquetra* (average $1.1 \times 10^6 \text{ cells L}^{-1}$, 78% of the total phytoplankton carbon biomass during the day, 31% at night) and *Aphanizomenon flos-aquae* ($1 \times 10^5 \text{ } 100\text{-}\mu\text{m}$ filaments L^{-1} , 4% during the day, 20% at night). The length and width of the *H. triquetra* cells measured microscopically from the surface samples were $23.7 \pm 2.3 \mu\text{m}$ and $15.9 \pm 1.73 \mu\text{m}$ ($n = 1,150$).

During the first survey and the first anchor station study, before the DCM was observed, the boundary of the layer with substantial chlorophyll concentration ($>1 \text{ mg Chl } a \text{ m}^{-3}$) extended to 10–20 m depth (Figs. 4a, 6a). The vertical and horizontal distribution of Chl *a* was patchy, but there was a tendency for the chlorophyll-containing layer to deepen through the pycnocline during the night (Fig. 6a,b,d).

During the second and third anchor station studies, the DCM was at about 30 m depth (Fig. 6b,d). The vertical distribution of *H. triquetra* abundance also showed higher

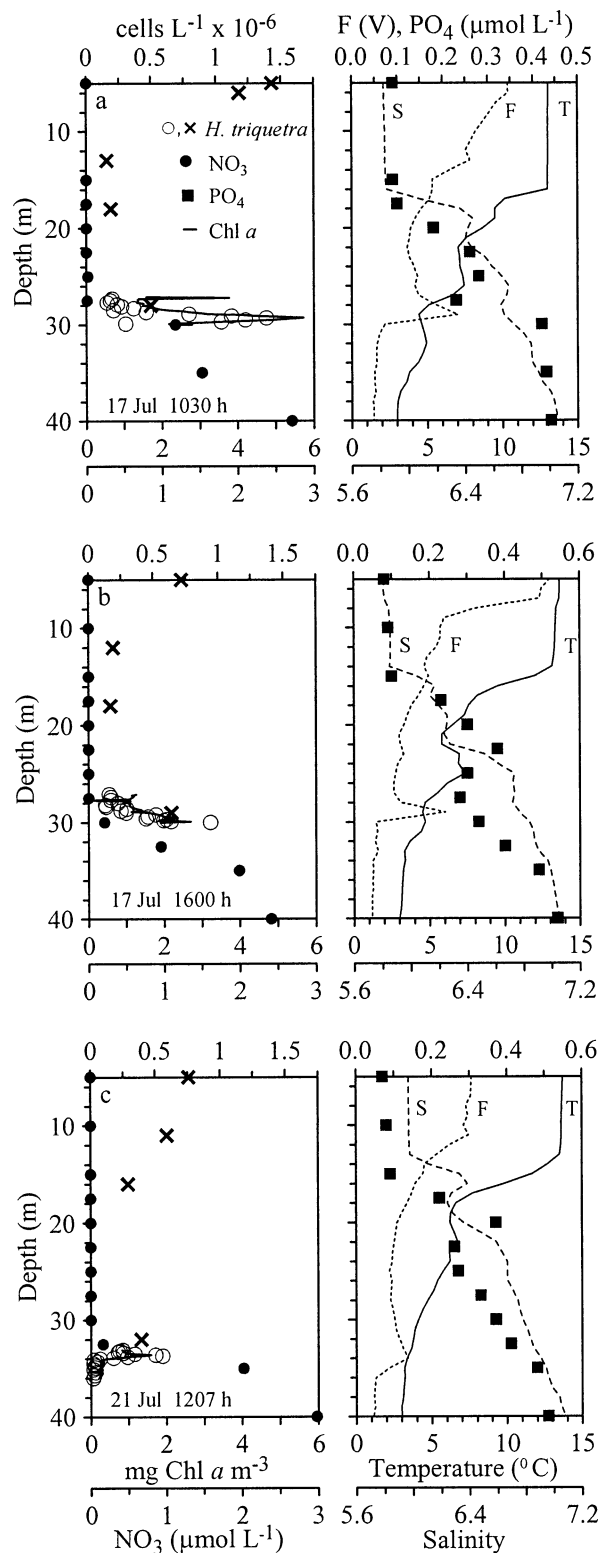


Fig. 8. Vertical profiles of *H. triquetra* abundance, nitrate, phosphate, Chl *a* from samples, salinity (S), fluorescence (F), and temperature (T) on (a, b) 17 July and (c) 21 July at the anchor station. Open circles represent the *H. triquetra* abundance counted from samples taken with the decimeter-scale sampler. Chl *a* is measured from the same samples.

values in the DCM than in the intermediate layer between the DCM and the upper layer (Fig. 8). The decimeter-scale vertical distributions of *H. triquetra* in the DCM layer demonstrated the accumulation of *H. triquetra* in the top of the nitracline (Fig. 8a–c). In the DCM, *H. triquetra* dominated (maximum detected abundance 1.6×10^6 cells L⁻¹), with a minor contribution of *Dinophysis acuminata* ($\sim 4 \times 10^3$ cells L⁻¹) and *Dinophysis norvegica* ($< 1 \times 10^3$ cells L⁻¹), and with a negligible contribution by any other species. This was also expressed in the good correlation between the abundance of *H. triquetra* and Chl *a* estimated from the DCM samples ($r^2 = 0.78$, $n = 48$, $p < 0.007$).

A good correlation ($r^2 = 0.62$, $p < 0.0001$) was found between the nitracline depth and the DCM depth, estimated from fluorescence profiles. The DCM moved relative to the nitracline; it was first situated at the top of the nitracline and, later, about few meters deeper (Fig. 6b,c).

In the DCM, particles 21–29 μm in length and 13–17 μm in width dominated. These dimensions correspond to the size of *H. triquetra* cells measured from the surface layer samples and to the diameter mode of 19 μm found in the monospecific culture. In the culture, the cell density N_c (cells ml⁻¹) correlated well with the number of particles (Q) measured by the PSA in the size range from 12 to 30 μm according to the following relation: $N_c = 2.14 \times 10^4 \times Q_{12-30\mu\text{m}}$ ($r^2 = 0.97$). The 18–30- μm size particle distribution measured in situ on 17 July also correlated with Chl *a* (cf. Fig. 6b,c); that is, the DCM contained mainly particles of the same size as *H. triquetra*. The average calculated cell density from the PSA measurements in the DCM was 1.2×10^6 cells L⁻¹. This value is in accordance with the abundance of *H. triquetra* determined from samples. No significant correlation between in vivo fluorescence and particles from 0.7 to 18 μm and $> 30 \mu\text{m}$ was found.

Comparison of the density of particles in the 12–30- μm size range and the synchronously measured in vivo fluorescence in the DCM led to the estimate of Chl *a* content of 3.3 pg cell⁻¹ ($n = 47$; $r^2 = 0.95$). In samples taken from the DCM, the content varied from 1.5 to 7.2 pg Chl *a* cell⁻¹, with 40% of the measurements between 3 and 4.5 pg Chl *a* cell⁻¹.

Primary production samples taken from the DCM layer and incubated in the surface illumination revealed that the DCM population was living and healthy, as it started to photosynthesize actively when exposed to illumination (Fig. 9).

Turbulence and chlorophyll fluxes at the anchor station—The three sets of turbulence data were obtained under different wind forcing conditions. Near-inertial waves generated by the passage of wind fronts during the first and third anchor stations contributed considerably to the vertical shear of current velocity; that is, it enhanced the turbulence level in the water column below the pycnocline. During the second anchor station, the wind was weak and the contribution from the near-inertial waves to turbulence production was minor. Stratification weakened and chlorophyll concentration decreased during the course of measurements at the anchor station (Fig. 10a). The mean eddy coefficients decreased from high values at the bottom of the mixed layer to low values in the pycnocline at 16–19 m depth, and they re-

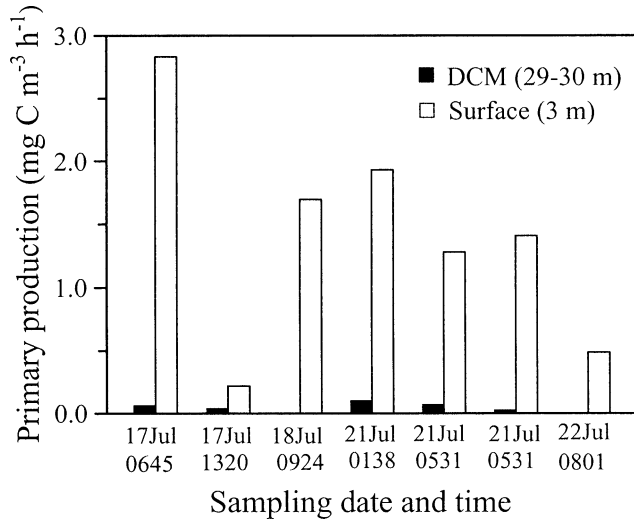


Fig. 9. Primary production ($\text{mg C m}^{-3} \text{ h}^{-1}$) measurements for samples taken from the DCM on 17, 18, 21, and 22 July at the anchor station. Filled bars represent incubation in the DCM depth (29–30 m) and open bars in the surface layer (3 m).

mained moderately variable, within the range of 10^{-5} – $10^{-4} \text{ m}^2 \text{ s}^{-1}$, in the water column below 20 m depth (Fig. 10b). Calculation of fluxes showed a downward mixing of chlorophyll (i.e., negative values of fluxes) in the bottom of the chlorophyll-containing layer for all three anchor stations (Fig. 10c). During the third anchor station, the maximum downward flux was smaller and situated deeper, in accordance with the averaged chlorophyll profile. In the DCM layer, chlorophyll fluxes were higher (up to $\pm 0.5 \times 10^{-5} \text{ mg Chl } a \text{ m}^{-2} \text{ s}^{-1}$ or $\pm 0.4 \text{ mg Chl } a \text{ m}^{-2} \text{ d}^{-1}$) in the lower boundary of the DCM than in the upper boundary. The calculated fluxes are estimates without accounting for the mobility of cells, which is especially important for the DCM formed by *H. triquetra*.

Characteristics of the DCM—Very few and weak signatures of the DCM were detected during the first mapping on 13–14 July in the eastern part of the study area. Already pronounced DCM layers were observed during the second anchor station on 17 July (Fig. 6b) and during the second mapping on 17–18 July (Table 2) in the same water, which meanwhile had advected continuously westward. Afterwards, the DCM was also mainly related to this water mass and only occasionally to the coastal cold water (Fig. 5). The warmer water in the southern part of the area was almost free of the DCM. All the DCM parameters were characterized by high horizontal variability, which was expressed in the large standard deviations (Table 2).

The mean thickness of the DCM (5–6 m) increased until 24 July, after which it decreased. Mean peak chlorophyll concentration values were a little less than $2 \text{ mg Chl } a \text{ m}^{-3}$, except for the next-to-last mapping when it was $2.5 \text{ mg Chl } a \text{ m}^{-3}$. The latter concentration can be explained by the presence of an anomalous patch of the DCM that had very high peak values in the SW corner of the area. The highest value, $10.1 \text{ mg Chl } a \text{ m}^{-3}$, was found only in this patch. The DCM sank $\sim 5 \text{ m}$ during the course of the study.

The amount of chlorophyll contained in the DCM was highest during the survey on 23–24 July, showing a 1.6-fold increase between 17 and 24 July; this was in accordance with the increase of both the mean chlorophyll maximum value and thickness (Table 2). A decrease of chlorophyll-related mean parameters in the last mapping on 26–27 July indicate that the DCM was then in a stage of retrogression. In order to compare the amount of chlorophyll contained in the DCM with the amount of chlorophyll in the water column above, the survey mean chlorophyll content (Chl_{0-25}) in the layer from surface to 25 m depth was calculated (Table 2). The survey mean amount of chlorophyll contained in the DCM formed 6–10% of the survey mean chlorophyll content in the water column above 25 m depth. The percentage was the highest for the survey on 23–24 July.

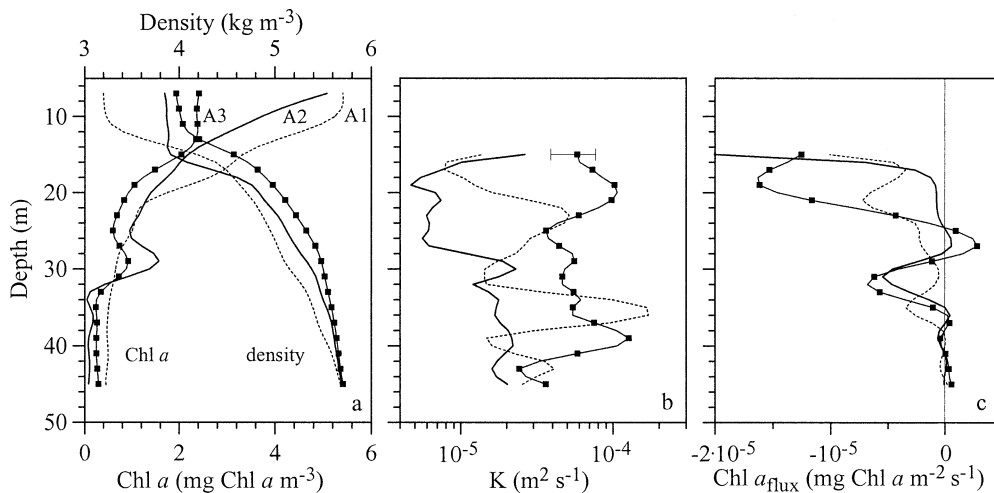


Fig. 10. Averaged over the sampling period, vertical profiles of (a) chlorophyll concentration and density; (b) eddy coefficient, K ; and (b, c) chlorophyll flux, $\text{Chl } a_{\text{flux}}$ on 14–15 July (dotted line), 17 July (bold line), and 21 July (line with filled squares) at the anchor station.

Table 2. Statistics of the DCM parameters estimated from data collected during mesoscale surveys (survey mean \pm SD). DCM parameters are estimated according to the definition in Fig. 2. In the last row is the survey mean (\pm SD) chlorophyll content in the water column from the surface to 25 m depth.

Parameter	17–18 Jul	19–20 Jul	22–23 Jul	23–24 Jul	26–27 Jul
Number of DCM layers	66	173	131	133	86
Maximum Chl _{max} (mg Chl <i>a</i> m ⁻³)	7.4	8.3	4.8	10.1	9.7
Chl _{max} (mg Chl <i>a</i> m ⁻³)	1.7 \pm 0.7	1.8 \pm 0.6	1.7 \pm 0.5	2.5 \pm 0.9	1.6 \pm 0.7
Chl _{con} (mg Chl <i>a</i> m ⁻²)	4.7 \pm 3.8	4.5 \pm 2.6	5.3 \pm 2.9	7.8 \pm 4.0	4.1 \pm 2.8
Depth (m)	30.1 \pm 2.0	33.8 \pm 3.3	34.7 \pm 3.1	35.5 \pm 2.4	35.7 \pm 3.5
Temperature (°C)	4.8 \pm 0.8	4.1 \pm 0.7	4.3 \pm 1.3	4.4 \pm 1.3	5.4 \pm 2.2
Salinity	6.8 \pm 0.1	6.9 \pm 0.1	6.9 \pm 0.1	6.9 \pm 0.1	6.9 \pm 0.1
Thickness, <i>h</i> (m)	4.9 \pm 2.9	4.7 \pm 2.3	5.6 \pm 2.6	6.2 \pm 3.1	4.8 \pm 2.6
Chl ₀₋₂₅ (mg Chl <i>a</i> m ⁻²)	74.4 \pm 14.6	70.6 \pm 13.5	80.9 \pm 14.9	79.2 \pm 15.6	73.4 \pm 12.8

Maintenance of dark fluorescence—Experiments performed with a pure culture of *H. triquetra* (7×10^4 cells ml⁻¹) in darkness revealed that the species was able to maintain about half of the starting concentration for a period of 18 d. During the first week, a rapid reduction in chlorophyll concentration from 5.2 pg Chl *a* cell⁻¹ to ~ 3 pg Chl *a* cell⁻¹ occurred (Fig. 11). 40% of the values measured in the DCM (3–4.5 pg Chl *a* cell⁻¹) were observed in vitro between days 3 and 7 of incubation. Cells adapted to subdued light and maintained their in vivo fluorescence between 3 and 4 mg Chl *a* m⁻³ for 7 d despite the strong decrease in total chlorophyll. During the next 11 d, the chlorophyll concentration decreased from ~ 3 to 2 pg Chl *a* cell⁻¹ and fluorescence from 3–4 to ~ 1.5 mg Chl *a* m⁻³.

Basinwide distribution of Heterocapsa triquetra—The measurements performed aboard the ferry *Finnjet* by Algeline along the transect between longitudes 20°E and 25°E showed that the amount of Chl *a* increased threefold between 9 June and 4 August (Fig. 12). The highest Chl *a* levels and patchiness were observed in the Gulf of Finland (i.e., east from longitude 22°E). In June, the amount of *H. triquetra* was negligible both in the northern Baltic proper and in the

Gulf of Finland. In early July, the species started to increase. It became dominant (ranking = 5) in the Gulf of Finland, but it remained sparse in the northern Baltic proper (ranking = 0, 1, 2). Measurements performed aboard the ferry *Wasa Queen* by Algeline on the Helsinki–Tallinn route (Fig. 1b) confirmed that the bloom developed on the northern side of the Gulf (data not shown).

Discussion

The main problem to solve is whether the DCM resulted from transport caused by physical processes or was created by vertically migrating *H. triquetra* cells as a response to the changing environmental conditions.

The DCM appeared in the water mass flowing out of the Gulf along the Finnish coast. The open Gulf water that was occasionally observed in the southern part of the study area lacked the DCM (Fig. 5; 19–20 and 26–27 July). The temperature in the DCM layer was low (the survey mean temperature varied between 4.1 and 5.4°C; Table 2). Low temperature excludes the possibility that the DCM was caused by the flow of water masses from the euphotic layer along sloping isopycnal surfaces. Temperature–salinity (T,S) diagrams of the CTD series at the anchor station on 17 and 21 July (Fig. 13) showed that the large variability of temperature and salinity fields was caused mainly by intrusions. The cold intrusions, likely originating from inshore regions, were phosphate-rich but contained no maxima on fluorescence profiles (Fig. 8). The DCM was situated deeper (Fig. 8), had a higher density (Figs. 4c,d, 13; Table 2), and was not related to the intrusive layering. These observations suggest that the DCM was not solely the result of physical forcing.

Diel vertical migration of H. triquetra—It is well known that many dinoflagellate species exhibit diel vertical migration related to environmental factors, such as irradiance and nutrient starvation or depletion (Cullen and MacIntyre 1998). Swimming speeds ranging between 0.2 and 2.16 m h⁻¹ have been reported for vertically migrating dinoflagellates (Levandowsky and Kaneta 1987). Periods of vertical migration longer than a day have been reported for the dinoflagellate *Pyrocystis* by Rivkin et al. (1984). The actual mechanisms of vertical migration (e.g., induction, cessation, trajectory, speed) might involve phototactical, chemotactical,

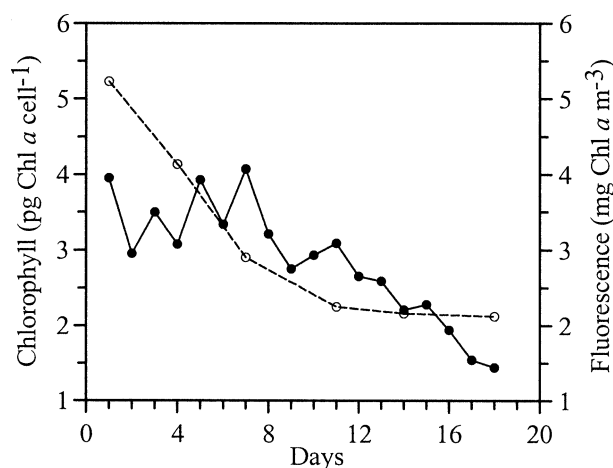


Fig. 11. Chlorophyll concentration (pg Chl *a* cell⁻¹, open circles) of a pure culture of *H. triquetra* grown in darkness for 18 d and measured by extraction of Chl *a* and in vivo fluorescence (mg Chl *a* m⁻³, filled circles).

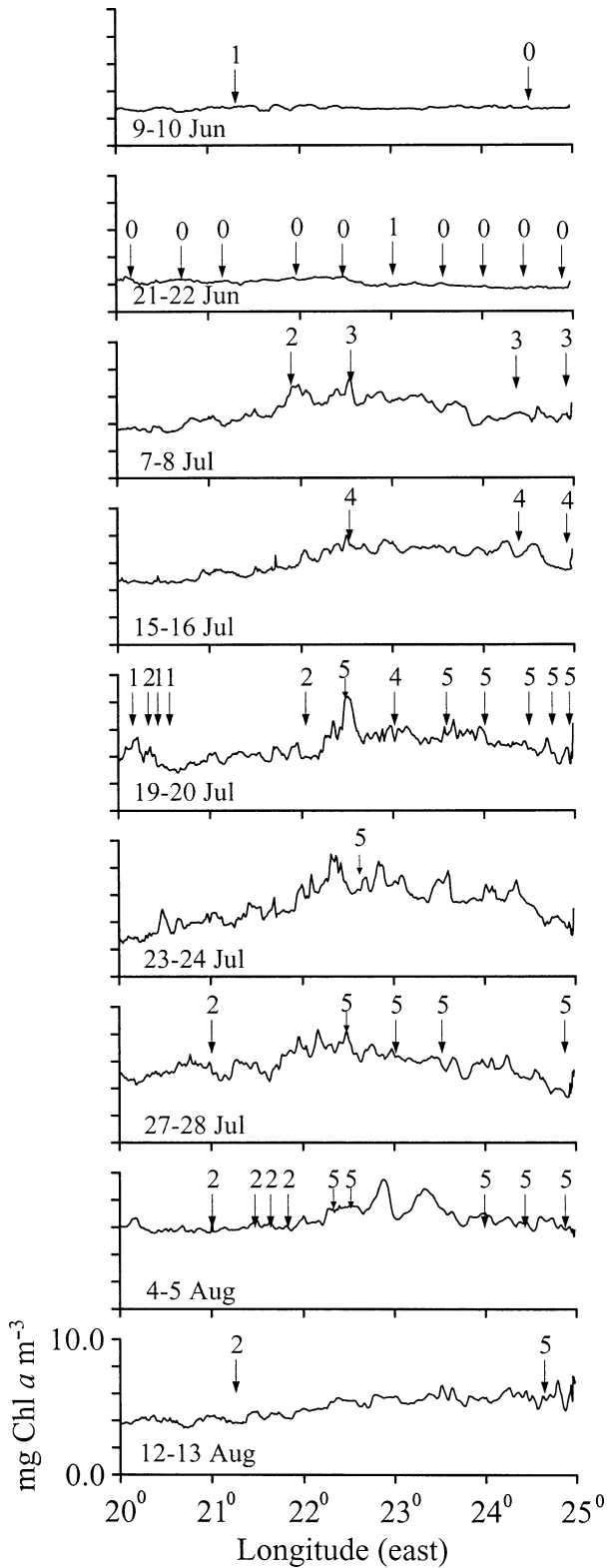


Fig. 12. Chl *a* (line) and the semiquantitative ranking of the abundance of *H. triquetra* at 5 m depth along the Algaline transect (20°–25°E) on June–August 1998. Arrows with numbers indicate phytoplankton sampling locations and rankings: 5, very abundant, dominant; 4, abundant; 3, scattered; 2, sparse; 1, very sparse.

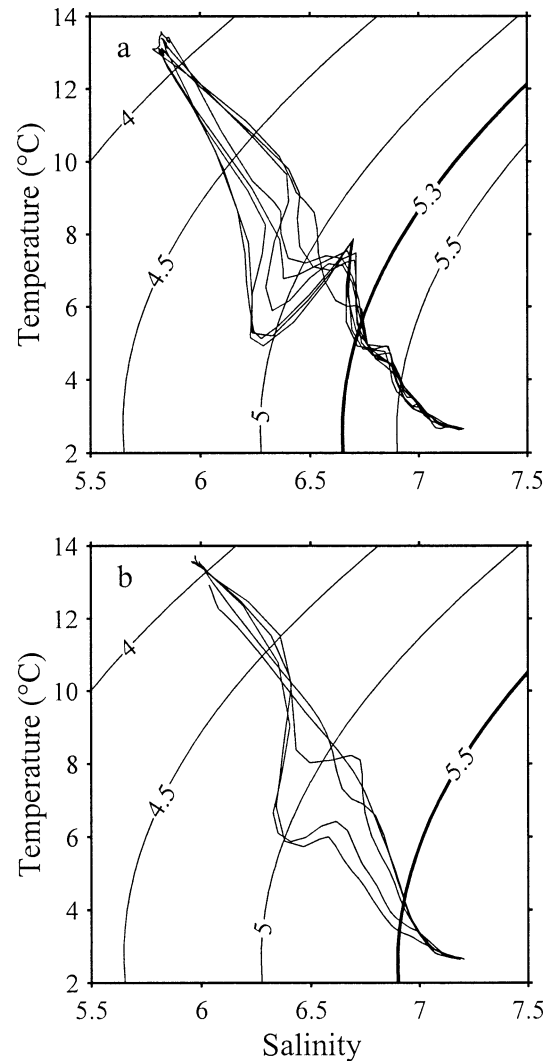


Fig. 13. T,S curves on (a) 17 July and (b) 21 July at the anchor station. Bold isopycnals correspond approximately to the density at the DCM depths.

and geotactical responses. Yet the physiological mechanisms behind the migratory behavior are unknown, and the taxis combinations might be species specific (Kamykowski et al. 1998a). Phototactic behavior of *H. triquetra* has been demonstrated both in the laboratory (Braarud and Pappas 1951) and in the field (Anderson and Stolzenbach 1985).

The vertical and horizontal distribution of Chl *a* was remarkably patchy during our observations. T,S diagrams also point to the large spatial variability of water column properties, partly caused by intrusions, in the upper 25-m layer (Fig. 13). This masks the vertical changes in the time series of chlorophyll profiles measured at the anchor station. However, that *H. triquetra* was performing diel vertical migration is suggested by the lower percentage of *H. triquetra* of the total phytoplankton biomass in the surface layer during the night compared to the day and by a tendency of the Chl *a*-containing layer to protrude through the pycnocline at night (Fig. 6a,b,d).

Red tide formed by H. triquetra—The large-scale distribution of *H. triquetra* in the northern Baltic Sea (Fig. 12) revealed that the bloom started in the beginning of July, ~2 weeks before the beginning of our cruise. The spring bloom of phytoplankton in the Gulf of Finland is nitrogen limited; therefore, during the time of the bloom initiation, the euphotic layer is usually nitrogen depleted.

In the beginning of our cruise, the total amount of Chl *a* above 25 m was ~70 mg Chl *a* m⁻² (Table 2), with *H. triquetra* being approximately half of the total phytoplankton biomass. Using the empirical C:Chl *a* ratio (C = 124 + 48 × Chl *a*, Heiskanen and Leppänen 1995) and the Redfield ratio (106 C:16 N:1 P), the amount of nitrogen in this *H. triquetra* biomass is ~23 mmol N m⁻². Approximately the same amount of nitrogen results if the calculation is made from cell abundances counted by a microscope: according to our data and the Algaline data (not shown), ~1 × 10⁶ *H. triquetra* cells L⁻¹ were observed at the beginning of our cruise. Using the cell carbon value of 149 pg C cell⁻¹ (Finnish Institute of Marine Research), this corresponds to 16 mmol N m⁻² in the 0–10-m layer.

Possible sources of nitrogen for this biomass formation include atmospheric deposition, nitrogen fixation, horizontal nitrogen input from loading, and entrainment of the nitrate below the thermocline. Because our cruise was carried out in the open sea far from nutrient-loading sources and during a period when the amount of nitrogen-fixing cyanobacteria was low, we believe that nitrogen fixation and nitrogen loading are unimportant. Atmospheric deposition of nitrogen, calculated from the yearly average for the Gulf of Finland (Kauppila et al. 2001) for a period of 2 weeks, is only ~1 mmol m⁻², which means that atmospheric deposition also cannot explain the bloom formation.

During the first anchor station study on 14–15 July, the nitracline was situated about 10 m deeper than the phosphocline; by the end of the samplings, the spacing between the two nutriclines was about 15 m. Nutrient sampling aboard RV *Aranda* during cruises in the same area during the second half of July 1994, 1997, and 1999 showed that the mean spacing between the phosphocline and the nitracline was about 5 m, and the nitracline depth was about 18 m (unpubl. data). In these years, instead of an *H. triquetra* bloom, a nitrogen-fixing cyanobacteria bloom was observed.

If the *H. triquetra* bloom had been formed on the basis of the nitrate pool below the thermocline, it would have resulted in a concentration decrease from 1–2 to 0 μmol L⁻¹ in the water column between the phosphocline and deepened nitracline. This corresponds with concentrations frequently observed in the Baltic Sea below the thermocline. Thus, the estimates of the amount of nitrogen required for a *H. triquetra* bloom support the conclusion that the red tide was formed on the basis of the nitrate pool below the thermocline, as reflected in the deepening of the nitracline.

Turbulence and maintenance of the DCM—Turbulent mixing plays two roles in the formation and maintenance of the DCM. First, it supports the downward migration of *H. triquetra* from the bottom of the euphotic layer. Second, turbulent mixing moves cells out of the top of the nitracline. To evaluate the swimming speed (*w*) necessary to maintain

the DCM, we used the relationship $w = K \partial \ln n_s / \partial z$ (Lande et al., 1989), where n_s is the species abundance. The largest change of *H. triquetra* abundance in the DCM, from 1.6×10^5 to 1.4×10^6 cells L⁻¹ in the 1.7-m depth interval, was observed on 17 July (Fig. 8a). This observation, along with an eddy coefficient of $K = 2 \times 10^{-5}$ m² s⁻¹ (Fig. 11b), gives a necessary speed of 0.1 m h⁻¹, which is much less than the swimming speed of *H. triquetra* of ~1 m h⁻¹ (Anderson and Stolzenbach 1985). The passage of a wind front increases the turbulence and, correspondingly, the necessary speed *w*, but the swimming speed of *H. triquetra* was still sufficient to maintain the DCM. That is indirectly supported by the DCM statistics of the survey on 22–23 July (Table 2), after the second wind event, when the mean chlorophyll peak decreased little and thickness increased.

Physiological mechanisms leading to the development of the DCM—There are several reasons why the diel vertical migration of *H. triquetra* is not alone sufficient to explain the DCM development at the depth of 30–35 m, adjacent to the nitracline. First, the known extent of diel migration (about 10 m) of this species is likely insufficient to reach the nitracline. This suggests that as soon as the DCM started to develop, the downward migrating cells did not change their orientation according to the diel cycle. Second, the DCM was not observed before the fourth day of our study; thus, before that day, a trigger must have induced the daily migrating population to continue downward instead of returning to the surface layer. Third, the DCM developed in the Gulf water flowing out along the Finnish coast, whereas the southern part of the area lacked the DCM. Thus, there must have been a factor in that coastal area that triggered downward migration to extend deeper or that prevented the change in the cells' orientation.

Considerable evidence suggests that the vertical migration of dinoflagellates is physiologically mediated (Cullen and MacIntyre 1998). However, the actual mechanisms of the process are poorly resolved. In the present study, the major hydrophysical factor affecting the growth environment of plankton was the weak upwelling and turbulent mixing that fertilized the upper mixed layer with phosphate, while the nitrate reserves were too deep to be mobilized. It can be assumed that, in this situation, plankton cells experience a shortage of nitrogen in the presence of surplus phosphorus and thus become nitrogen starved. Migrating dinoflagellates are known to be especially sensitive to nitrate (Cullen and Horrigan 1981; MacIntyre et al. 1997).

It was notable that the DCM developed when the migrating cells changed their swimming behavior; instead of returning to the surface, their migration continued downward. It has been suggested that the orientation of swimming cells is regulated physiologically through differential accumulation of metabolic products in different sides of the cell (Lieberman et al. 1994; Kamykowski 1995; Cullen and MacIntyre 1998; Kamykowski et al. 1998b).

It is also possible that a nitrate concentration gradient detectable by the cells in the water column guides the swimming direction of nitrogen-starved cells. Dinoflagellates are known to exhibit chemotactical responses to very low concentrations of various compounds (Levandowsky and Kaneta

1987). Turbulent mixing might entrain the nitracline and create and maintain small gradients in the water column above the deep nitracline. To evaluate the possibility of a chemotactical response, we used the measured eddy coefficients, nitrate profiles, and the simplified diffusion equation $\partial(\text{NO}_3)/\partial t = \partial/\partial z(K \partial(\text{NO}_3)/\partial z)$, where t is time and the z -axis is positive upward. Integration of this equation for 1 d indicates that turbulence could have resulted in concentrations of $1-3 \times 10^{-4} \mu\text{mol L}^{-1}$ to the depths of 19, 24, and 18 m for the first, second, and third anchor stations, respectively. If we assume that the diel migration was ~ 10 m, the dinoflagellate population could therefore have sensed the nitrate concentration gradient during a diel migratory cycle. Thus, the migratory behavior and the DCM formation can be, at least partly, explained by chemotaxis.

In order to utilize nitrates in the deep layer, uptake by the species has to take place in the dark. Paasche et al. (1984) revealed that, unlike the case for many other dinoflagellates, uptake of nitrate by *H. triquetra* is as efficient in the dark as in the light. Assimilation of nitrate requires carbohydrates that have been stored during the light period (Cullen 1985); therefore, there must be a time limit that a species can remain in darkness in the DCM. Based on the Chl *a* quota, we estimated that 25% of the cells resided less than 2 d in the DCM, and the average residence time was between 3 and 6 d (40% of the observations). Maintenance of the in vivo fluorescence at a level close to that of light-reared cells would explain the ability of this population to readily photosynthesize immediately when brought to the surface (Fig. 9). An additional functional capability that might help cells survive in darkness is their potential phagotrophy, as reported by Legendre et al. (1998).

Ecological advantages provided by vertical migration—The ecological advantage provided by vertical migration is the ability to utilize nutrient reserves deep in the water column when the surface layer is nutrient depleted. The bloom of *H. triquetra* developed in July 1998, when blooms of nitrogen-fixing cyanobacteria normally occur (e.g., Kononen et al. 1996). The red tide was also reported by Lindholm and Nummelin (1999) in a coastal inlet in the Archipelago Sea. Blooms of cyanobacteria in the Baltic Sea result from high phosphate at or near the surface (Niemi 1979) and on the nitrogen fixation capacity of cyanobacteria. Summer 1998 was exceptionally cold and windy in the Gulf area and bloom-forming cyanobacteria did not become abundant. As in the present study, in the relatively cold July 1996, we also observed a DCM and a bloom of *H. triquetra* rather than the typical cyanobacterial bloom at the entrance to the Gulf of Finland (Kononen et al. 1999; Pavelson et al. 1999). It seems likely, then, that high turbulence and low water temperature during windy summers prevent blooms of nitrogen-fixing cyanobacteria. In such situations, migratory species that are able to exploit the deeper nitrate reserves have an advantage.

The 2-week field study described in this paper confirmed that the DCM was created as a combined effect of upwelling and the physiologically regulated migration of *H. triquetra*. We conclude that the bloom initiation and the nitracline deepening occurred primarily as a result of diel vertical mi-

gration, which allowed this species to access nitrate deep in the water column. When the nitracline deepened, the formation of DCM was stimulated by upwelling, which provided phosphate and modified the physiological status and swimming behavior of cells, and by turbulence, which created nitrate gradients in the water column above the nitracline.

The red tide development by *H. triquetra* and the observed DCM formation resulted when low temperature, high wind speed, and turbulence prevented the development of cyanobacteria, despite the presence of surplus phosphate in the surface layer. The results confirmed that the red tide formation is accentuated in areas where and when coastal upwelling events repeatedly enrich the surface layer with new phosphate.

References

- AGAWIN, N. S. R., AND A. AGUSTI. 1997. Abundance, frequency of dividing cells and growth rates of *Synechococcus* sp. (cyanobacteria) in the stratified Northwest Mediterranean Sea. *J. Plankton Res.* **19**: 1599–1615.
- ANDERSON, D. M., AND K. D. STOLZENBACH. 1985. Selective retention of two dinoflagellates in a well-mixed estuarine embayment: The importance of diel vertical migration and surface avoidance. *Mar. Ecol. Prog. Ser.* **25**: 39–50.
- [BMEPC] BALTIC MARINE ENVIRONMENT PROTECTION COMMISSION. 1983. Guidelines for the Baltic monitoring programme for the second stage. Baltic Sea Environment Proceedings No. 12. Baltic Marine Environment Protection Commission, Helsinki.
- BRAARUD T., AND I. PAPPAS. 1951. Experimental studies on the dinoflagellate *Peridinium triquetrum* (Ehrenberg) Lebour. *Norse Vidensk-Akad. Oslo. Avh I Mat Naturv Klasse* **2**: 1–23.
- CARPENTER, E. J., S. JANSON, R. BOJE, F. POLLEHNE, AND J. CHANG. 1995. The dinoflagellate *Dinophysis norvegica*: Biological and ecological observations in the Baltic Sea. *Eur. J. Phycol.* **30**: 1–9.
- CLAUSTRE, H., AND OTHERS. 1999. Variability in particle attenuation and chlorophyll fluorescence in the Tropical Pacific: Scales, patterns and biochemical implications. *J. Geophys. Res., C* **104**: 3401–3422.
- CULLEN, J. J. 1982. The deep chlorophyll maximum: Comparing vertical profiles of chlorophyll *a*. *Can. J. Fish. Aquat. Sci.* **39**: 791–803.
- . 1985. Diel vertical migration by dinoflagellates: Roles of carbohydrate metabolism and behavioural flexibility. *Cont. Mar. Sci.* **27**: 135–152.
- , AND S. G. HERRIGAN. 1981. Effect of nitrate on the diurnal vertical migration, carbon to nitrogen ratio and the photosynthetic capacity of the dinoflagellate *Gymnodinium splendens*. *Mar. Biol.* **62**: 81–89.
- , AND J. G. MACINTYRE. 1998. Behaviour, physiology and the niche of depth-regulating phytoplankton, p. 559–579. *In* D. M. Anderson, A. D. Cembella, and G. M. Hallegraeff [eds.], NATO ASI Series Vol. G41. Physiological ecology of phytoplankton. Springer-Verlag.
- DERENBACH, J. B., H. P. ASTHEIMER, AND H. LEACH. 1979. Vertical microscale distribution of phytoplankton in relation to the thermocline. *Mar. Ecol. Prog. Ser.* **1**: 187–193.
- EPPLEY, R. W., F. M. H. REID, J. J. CULLEN, C. D. WINANT, AND E. STEWART. 1984. Subsurface patch of dinoflagellate (*Ceratium tripos*) off Southern California: Patch length, growth rate,

- associated vertically migrating species. *Mar. Biol.* **80**: 207–214.
- GENTIEN, P., M. LUNVEN, M. LEHAITRE, AND J. L. DUVENT. 1995. In situ depth profiling of particle sizes. *Deep-Sea Res.* **42**: 1297–1312.
- . 1998. Bloom dynamics and ecophysiology of the *Gymnodinium mikimotoi* species complex, p. 155–173. In D. M. Anderson, and others [eds.], *Physiological ecology of harmful algal blooms*. Springer-Verlag.
- HEISKANEN, A.-S., AND J.-M. LEPPÄNEN. 1995. Estimation of export production in the coastal Baltic Sea: Effect of resuspension and microbial decomposition on sedimentation measurements. *Hydrobiologia* **316**: 211–224.
- KAMYKOWSKI, D. 1995. Trajectories of autotrophic marine dinoflagellates. *J. Phycol.* **31**: 200–208.
- , E. J. MILLIGAN, AND R. E. REED. 1998a. Relationships between geotaxis/phototaxis and diel vertical migration in autotrophic dinoflagellates. *J. Plankton Res.* **20**: 1781–1796.
- , ———, AND ———. 1998b. Biochemical relationships with orientation of the autotrophic dinoflagellate *Gymnodinium breve* under nutrient replete conditions. *Mar. Ecol. Prog. Ser.* **167**: 105–117.
- KAUPPILA, P., M. KORHONEN, H. PITKÄNEN, K. KENTTÄMIES, S. REKOLAINEN, AND P. KOTILAINEN. 2001. Loading of pollutants, p. 15–29. In P. Kauppila and S. Bäck [eds.], *The state of Finnish coastal waters in the 1990s*. The Finnish Environment 472. Finnish Environment Institute, Helsinki.
- KONONEN, K., J. KUPARINEN, K. MÄKELÄ, J. LAANEMETS, J. PAVELSON, AND S. NÖMMANN. 1996. Initiation of cyanobacterial blooms in a frontal region at the entrance to the Gulf of Finland, Baltic Sea. *Limnol. Oceanogr.* **41**: 98–112.
- , S. HÄLLFORS, M. KOKKONEN, H. KUOSA, J. LAANEMETS, AND J. PAVELSON. 1998. Development of a subsurface chlorophyll maximum at the entrance to the Gulf of Finland, Baltic Sea. *Limnol. Oceanogr.* **43**: 1089–1106.
- , M. HUTTUNEN, I. KANOSHINA, J. LAANEMETS, P. MOISANDER, AND J. PAVELSON. 1999. Spatial and temporal variability of a dinoflagellate–cyanobacterium community under a complex hydrodynamical influence: A case study at the entrance to the Gulf of Finland. *Mar. Ecol. Prog. Ser.* **186**: 43–57.
- KUOSA, H. 1990. Subsurface chlorophyll maximum in the northern Baltic Sea. *Arch. Hydrobiol.* **118**: 437–447.
- LANDE, R., W. K. W. LI, E. P. W. HORNET, AND A. M. WOOD. 1989. Phytoplankton growth rates estimated from the depth profiles of cell concentration and turbulent diffusion. *Deep-Sea Res.* **36**: 1141–1159.
- LEGRAND, C., E. GRANIELI, AND P. CARLSSON. 1998. Induced phagotrophy in the photosynthetic dinoflagellate *Heterocapsa triquetra*. *Mar. Ecol. Prog. Ser.* **15**: 65–75.
- LEPPÄNEN, J.-M., AND E. RANTAJÄRVI. 1995. Unattended recording of phytoplankton and supplemental parameters on board merchant ships—an alternative to the conventional algal monitoring programmes in the Baltic Sea, p. 719–724. In P. Lassus, G. Arzul, E. Erard-Le Denn, P. Gentien, and E. Mercaillere-Le Baut [eds.], *Harmful marine algal blooms*. Lavoisier.
- LEVANDOWSKY, M., AND P. KANETA. 1987. Behaviour in dinoflagellates, p. 360–397. In F. J. R. Taylor [ed.], *The biology of dinoflagellates*. Blackwell.
- LIEBERMAN, O. S., M. SHILO, AND J. VAN RIJN. 1994. The physiological ecology of a freshwater dinoflagellate bloom population: Vertical migration, nitrogen limitation, and nutrient uptake kinetics. *J. Phycol.* **30**: 964–971.
- LINDHOLM, T., AND C. NUMMELIN. 1999. Red tide of the dinoflagellate *Heterocapsa triquetra* in a ferry-mixed coastal inlet. *Hydrobiologia* **383**: 245–251.
- MACINTYRE, J. G., J. J. CULLEN, AND A. D. CEMBELLA. 1997. Vertical migration, nutrition and toxicity in the dinoflagellate *Alexandrium tamarense*. *Mar. Ecol. Prog. Ser.* **148**: 201–216.
- MACKEY, D. J., J. PARSLAW, H. W. HIGGINS, F. B. GRIFFITH, AND J. E. O’SULLIVAN. 1995. Plankton productivity and biomass in the western equatorial Pacific: Biological and physical controls. *Deep-Sea Res.* **42**: 499–533.
- MOUM, J. N., AND R. G. LUECK. 1985. Causes and implications of noise in oceanic dissipation measurements. *Deep-Sea Res.* **32**: 379–390.
- NIEMI, Å. 1979. Blue-green algal blooms and N:P ratio in the Baltic Sea. *Acta Bot. Fenn.* **110**: 57–61.
- OSBORN, T. 1980. Estimates of the local rate of vertical diffusion from dissipation measurements. *J. Phys. Oceanogr.* **10**: 83–89.
- PAASCHE, E., I. BRYCESON, AND K. TANGEN. 1984. Interspecific variation in dark nitrogen uptake by dinoflagellates. *J. Phycol.* **20**: 394–401.
- PAVELSON, J., K. KONONEN, AND J. LAANEMETS. 1999. Chlorophyll distribution patchiness caused by hydrodynamical processes: A case study in the Baltic Sea. *ICES J. Mar. Sci. (suppl.)* **56**: 87–99.
- PRANDKE, H., AND A. STIPS. 1998. Test measurements with an operational microstructure–turbulence profiler: Detection limit of dissipation rates. *Aquat. Sci.* **60**: 191–209.
- RIVKIN, R. B., E. SWIFT, W. H. BIGGLEY, AND M. A. VOYTEK. 1984. Growth and carbon uptake by natural populations of oceanic dinoflagellates *Pyrocystis noctiluca* and *Pyrocystis fusiformis*. *Deep-Sea Res.* **31**: 353–367.
- SCHAREK, R., M. LATASA, D. M. KARL, AND R. R. BIDIGARE. 1999. Temporal variations in diatom abundance and downward vertical fluxes in the oligotrophic North Pacific Gyre. *Deep-Sea Res.* **46**: 1051–1075.
- UTERMÖHL, H. 1958. Zur Vervollkommnung der quantitativen Phytoplanktonmetodik. *Mitt. Int. Verein. Limnol.* **9**: 1–38.
- VELDHUIS, M. J. C., AND G. W. KRAAY. 1990. Vertical distribution and pigment composition of a picoplanktonic prochlorophyte in the subtropical North Atlantic: A combined study of HPLC-analysis of pigments and flow cytometry. *Mar. Ecol. Prog. Ser.* **68**: 121–127.
- VENRICK, E. L., J. A. MCGOWAN, AND A. W. MANTYLA. 1973. Deep maxima of photosynthetic chlorophyll in the Pacific Ocean. *Fish. Bull.* **71**: 41–51.
- WASHBURN, L., AND OTHERS. 1991. Water mass subduction and the transport of phytoplankton in a coastal upwelling system. *J. Geophys. Res.* **96**: 14,927–14,945.

Received: 26 September 2001
 Amended: 11 September 2002
 Accepted: 29 September 2002